

also pBiPs were enriched for CRE consensus sequences, and were preferential targets for regulation by the transcription factors in the cAMP-dependent pathway (Figures 3B and 8 and Supplementary Figure S13). We reported previously that transcription of pancRNAs from pBiPs epigenetically activates partner tissue-specific genes (7,8,11). Consistent with previous reports that pancRNAs contribute to the establishment of cell identity via epigenetic regulation of tissue-specific gene expression, the expression levels of pancRNAs derived from pBiPs tended to be positively correlated with the expression levels of their partner mRNAs during differentiation of PC12 cells (Figure 3C). Furthermore, epigenetic activation via pancRNAs was confirmed here by the manipulation of the *pancNusap1* levels in PC12 cells (Figures 5–7). Thus, the present results provide the new insight that transcriptional regulation by means of pancRNAs provides adaptive advantages for CRE-mediated gene regulation. Considering that the number of pBiPs is almost 6-fold greater than the number of aBiPs, the impacts of pBiPs as important effectors of cAMP signals might be greater than those of aBiPs for coordinated activation of a fraction of cAMP-responsive genes.

The silencing of M-phase progression contributes to the establishment of an irreversibly differentiated state: implications for neuronal differentiation

We showed that regulation of cell-cycle-associated genes plays crucial roles in the process of irreversible differentiation of PC12 cells (Figures 5–7). The critical importance of maintaining the cell-cycle-arrested state in neurons is supported by studies on somatic cell nuclear transfer. When nuclei of adult cortical neurons are used as donors, the majority of reconstructed mouse oocytes are arrested at the first mitotic cleavage with abnormal chromosome condensation (40), whereas reconstructed oocytes cloned from nuclei of other types of differentiated somatic cells, such as cumulus cells (41) and tail tip fibroblasts (42), show much greater developmental potential. Because the cell cycle of neurons is arrested at G0 phase, many studies have focused on the relationship between neuronal differentiation and inhibition of G1/S-phase progression (43,44). For example, neuronal differentiation of mouse neural stem cells is enhanced by double knockout of G1/S-phase-progression-associated genes *Cdk2* and *Cdk4* (45). Similarly, Ndiff PC12 cells have been widely used as an *in vitro* model for investigating the relationship between G1/S-phase inhibition and neurite outgrowth. In fact, like the Cdk2 protein level, the level of Pcna and phosphorylated retinoblastoma protein, also known as G1/S-phase-progression-associated proteins, are downregulated in Ndiff PC12 cells (46–48), suggesting that G1/S-phase inhibition also occurs in reversibly differentiated Ndiff PC12 cells.

In addition, several lines of evidence indicate that inhibition of M-phase-associated genes is involved in the functional differentiation of neurons (49,50). For example, reconstructed mouse oocytes cloned from nuclei of adult cortical neurons undergo abnormal cell cycle arrest at the first mitotic cleavage (40). In mouse neural progenitors, KD of an M-phase-progression-associated gene, doublecortin-like kinase, causes neuronal differentiation (51). Therefore, co-

ordinated regulation of G1/S-phase-progression-associated genes and M-phase-progression-associated genes seems to be important for neuronal differentiation. In this context, it is interesting to note that the expression of cell-cycle-associated genes, especially those related to G2/M-phase progression, remained high in Ndiff PC12 cells (Figure 2) and epigenetic silencing of M-phase-associated *Nusap1* could convert reversibly differentiated cells into irreversibly differentiated cells (Figure 5). Considering that inhibition of G1/S-phase progression is observed in reversibly differentiated Ndiff PC12 cells (Supplementary Figure S14), NGF and cAMP signalings appear to be strongly involved in G1/S- and G2/M-inhibition, respectively, for completing the differentiation of neurons. Our results suggested that irreversible/reversible PC12 differentiation could be a good model for further addressing the lncRNA-mediated mechanisms that link cell cycle regulation to irreversible differentiation.

The pancRNA repertoires are differentially utilized from the zygotic to the terminally differentiated stages

In this study, the RNA-seq method was utilized to test whether pancRNA-mediated gene activation mechanisms function in the terminal differentiation of the cells on a genome-wide scale, and the results confirmed this hypothesis (Figures 3, 5 and 6). Indeed, pancRNAs have been detected from more than a thousand promoter regions at a very early stage of life called zygotic gene activation (7). Previous reports have also shown that thousands of pancRNAs are transcribed in ES cells and various tissues (11,52). Thus, a non-negligible number of pancRNAs seem to be expressed in various contexts. Since pancRNAs and mRNAs exhibit coordinated expression changes not only in totipotent/pluripotent cells but also in terminally differentiated cells (Figure 3C), pancRNAs may be commonly utilized for gene activation from the zygotic to the terminally differentiated stage. Although we focused on a study of functional pancRNAs from the polyA⁺ and >200 bp ncRNA fraction in this study, other fractions of ncRNAs (e.g. polyA⁻, <200 bp) derived from the promoter of protein-coding genes may also function in transcriptional activation of their partner genes (37,53). The general usage of the pancRNA system over the course of life sheds light on the importance of gene-activation-associated ncRNAs as counterparts of gene-silencing ncRNAs, such as microRNA, which work at the post-transcriptional level. Studies of possible coordinated regulation with lncRNAs derived from enhancer regions, called eRNAs (32,54–59) would be the next step in elucidating the sequence-specific gene activation mechanisms in which ncRNA structurally recognizes genomic DNA.

Transcriptional silencing of *Nusap1* in response to extracellular differentiation stimuli is an important step of cAMP signaling toward terminal differentiation of PC12 cells

Nusap1 protein has a well-conserved microtubule-binding domain in its COOH terminus and a DNA-binding SAP domain in its NH2 terminus, and promotes the stabilization and crosslinking of microtubules near chromosomes

in metaphase/anaphase (60,61). *Nusap1* is highly expressed in proliferative tissues, and essential for M-phase progression. In cultured cell lines, KD of *Nusap1* causes severe mitotic defects with defective anaphase and cytokinesis (60), and knockout of *Nusap1* induces early embryonic lethality in mice (62). Like other cell cycle regulators, the protein level of *Nusap1* is under the regulation of a multisubunit E3 ubiquitin ligase, anaphase promoting complex/cyclosome, in proliferating cells (63). However, the mechanisms of transcriptional regulation of *Nusap1* in terminally differentiated cells are still unknown. In this study, we showed that reduced transcription of *Nusap1* via downregulation of *pancNusap1* in response to cAMP stimulation functions in the terminal differentiation of PC12 cells (Figures 5–8). These findings indicated that transcriptional silencing of *Nusap1* is a key mediator of cAMP signaling for terminal differentiation of PC12 cells. The epigenetic silencing by the concomitant reduction of *pancNusap1* by cAMP may further support the complete shut-down of neuronal cell division.

Possible molecular mechanism underlying *pancNusap1*-mediated epigenetic modification

We and others have reported that *pancRNA* promotes the assembly of an open chromatin conformation that includes histone acetylation, H3K4 methylation, H3K9/K27 demethylation and active DNA demethylation (7,8,12,64). Differently from these previous results, the present data indicated that the activation and reduction of *pancNusap1* expression increased and decreased the histone acetylation levels of the *Nusap1* promoter, respectively, but not the levels of histone methylation or DNA methylation (Figures 4–6, and Supplementary Figure S1). There are many reports indicating that functional lncRNAs recruit epigenetic modification complexes, such as histone methyltransferase myeloid/lymphoid or mixed-lineage leukemia (MLL) complex and the BER components at specific genomic locations (1,56,65–67). However there are no reports that prove the interaction of lncRNAs with histone acetyltransferase complex. Recently, nuclease-null Cas9-based transcriptional activation technology has revealed that artificial transcription initiation at an intergenic locus elevates H3K27ac levels (68). Furthermore, single living cell analysis has shown that recruitment of RNAPII occurs within a few minutes after histone acetylation at the glucocorticoid receptor gene locus (69). Given these reports, one possible scenario is that transcription initiation of *pancNusap1* primary causes histone acetylation at the *Nusap1* promoter and thus enhances specific gene expression there.

Interestingly, we and others have reported that only antisense *pancRNAs* are associated with chromatin, and *pancRNA*-mediated transcriptional activation occurs in a strand-specific manner (8,64). Consistent with these reports, the transcriptional direction of *pancNusap1* is important for *pancNusap1*-mediated histone acetylation (Figure 6). In this context, it is worthwhile to note that *pancNusap1* has a G-rich sequence (Supplementary Figure S15). Because guanine (G)-rich RNA that hybridizes with single-stranded cytosine (C)-rich complementary DNA forms a thermodynamically stable DNA:RNA hybrid structure, known as an R-loop structure (70,71), the sequence-

dependent stability of R-loops may explain the increase of histone acetylation by *pancNusap1*. Further studies will be needed to unravel the molecular mechanisms that determine the sequential epigenetic changes induced by *pancRNA*-mediated histone acetylation.

In conclusion, *pancRNA*-mediated histone acetylation contributes to the establishment of PC12 cells' stimulation-induced transcription status during the irreversible differentiation process.

DATA AVAILABILITY

RNA-seq data have been deposited in the DDBJ Sequence Read Archive (DRA) under accession number DRA004148.

SUPPLEMENTARY DATA

Supplementary Data are available at NAR Online.

ACKNOWLEDGEMENT

We thank Osamu Nishimura and Masahiro Uesaka for providing advice about transcriptome analysis; Nobuhiko Hamazaki and Hirofumi Noguchi for scientific insights and suggestions throughout the study; Katsuhide Igarashi, Hideyuki Nakashima, Tsukasa Sanosaka and Sayako Katada for experimental advice; and Elizabeth Nakajima for proofreading the manuscript.

FUNDING

Japan Society for the Promotion of Science [15H04603; 24380158 to T. I., 241544 to N. Y.]; Global COE program [A06 to Kyoto University]; Scientific Research on Innovative Areas 'Genome Science' from the Ministry of Education, Culture, Sports, Science and Technology (MEXT) [221S0002 to T.I.]. Funding for open access charge: Japan Society for the Promotion of Science [15H04603, 24380158 to T. I., 241544 to N. Y.]; Global COE program [A06 to Kyoto University]; Scientific Research on Innovative Areas 'Genome Science' from the Ministry of Education, Culture, Sports, Science and Technology (MEXT) [221S0002].

Conflict of interest statement. None declared.

REFERENCES

- Guttman, M., Donaghey, J., Carey, B.W., Garber, M., Grenier, J.K., Munson, G., Young, G., Lucas, A.B., Ach, R., Bruhn, L. *et al.* (2011) lincRNAs act in the circuitry controlling pluripotency and differentiation. *Nature*, **477**, 295–300.
- Carrieri, C., Cimatti, L., Biagioli, M., Beugnet, A., Zucchelli, S., Fedele, S., Pesce, E., Ferrer, I., Collavin, L., Santoro, C. *et al.* (2012) Long non-coding antisense RNA controls Uchl1 translation through an embedded SINEB2 repeat. *Nature*, **491**, 454–457.
- Ng, S.-Y., Bogu, G.K., Soh, B.S. and Stanton, L.W. (2013) The long noncoding RNA RMST interacts with SOX2 to regulate neurogenesis. *Mol. Cell*, **51**, 349–359.
- Herzog, V.A., Lempradl, A., Trupke, J., Okulski, H., Altmutter, C., Ruge, F., Boidol, B., Kubicek, S., Schmauss, G., Aumayr, K. *et al.* (2014) A strand-specific switch in noncoding transcription switches the function of a Polycomb/Trithorax response element. *Nat. Genet.*, **46**, 973–981.

5. Ting, A.H., Schuebel, K.E., Herman, J.G. and Baylin, S.B. (2005) Short double-stranded RNA induces transcriptional gene silencing in human cancer cells in the absence of DNA methylation. *Nat. Genet.*, **37**, 906–910.
6. Gupta, R.A., Shah, N., Wang, K.C., Kim, J., Horlings, H.M., Wong, D.J., Tsai, M.-C., Hung, T., Argani, P., Rinn, J.L. *et al.* (2010) Long non-coding RNA HOTAIR reprograms chromatin state to promote cancer metastasis. *Nature*, **464**, 1071–1076.
7. Hamazaki, N., Uesaka, M., Nakashima, K., Agata, K. and Imamura, T. (2015) Gene activation-associated long noncoding RNAs function in mouse preimplantation development. *Development*, **142**, 910–920.
8. Tomikawa, J., Shimokawa, H., Uesaka, M., Yamamoto, N., Mori, Y., Tsukamura, H., Maeda, K.-I. and Imamura, T. (2011) Single-stranded noncoding RNAs mediate local epigenetic alterations at gene promoters in rat cell lines. *J. Biol. Chem.*, **286**, 34788–34799.
9. Sigova, A.A., Abraham, B.J., Ji, X., Molinie, B., Hannett, N.M., Guo, Y.E., Jangi, M., Giallourakis, C.C., Sharp, P.A. and Young, R.A. (2015) Transcription factor trapping by RNA in gene regulatory elements. *Science*, **350**, 978–981.
10. Ravasi, T., Suzuki, H., Pang, K.C., Katayama, S., Furuno, M., Okunishi, R., Fukuda, S., Ru, K., Frith, M.C., Gongora, M.M. *et al.* (2006) Experimental validation of the regulated expression of large numbers of non-coding RNAs from the mouse genome. *Genome Res.*, **16**, 11–19.
11. Uesaka, M., Nishimura, O., Go, Y., Nakashima, K., Agata, K. and Imamura, T. (2014) Bidirectional promoters are the major source of gene activation-associated non-coding RNAs in mammals. *BMC Genomics*, **15**, 35.
12. Imamura, T., Yamamoto, S., Ohgane, J., Hattori, N., Tanaka, S. and Shiota, K. (2004) Non-coding RNA directed DNA demethylation of Sphk1 CpG island. *Biochem. Biophys. Res. Commun.*, **322**, 593–600.
13. Hegedus, B., Dasgupta, B., Shin, J.E., Emmett, R.J., Hart-Mahon, E.K., Elghazi, L., Bernal-Mizrachi, E. and Gutmann, D.H. (2007) Neurofibromatosis-1 regulates neuronal and glial cell differentiation from neuroglial progenitors in vivo by both cAMP- and Ras-dependent mechanisms. *Cell Stem Cell*, **1**, 443–457.
14. Zahir, T., Chen, Y.F., MacDonald, J.F., Leipzig, N., Tator, C.H. and Shoichet, M.S. (2009) Neural stem/progenitor cells differentiate in vitro to neurons by the combined action of dibutyl cAMP and interferon-gamma. *Stem Cells Dev.*, **18**, 1423–1432.
15. Impey, S., McCorkle, S.R., Cha-Molstad, H., Dwyer, J.M., Yochum, G.S., Boss, J.M., McWeeney, S., Dunn, J.J., Mandel, G. and Goodman, R.H. (2004) Defining the CREB regulon: a genome-wide analysis of transcription factor regulatory regions. *Cell*, **119**, 1041–1054.
16. Cha-Molstad, H., Keller, D.M., Yochum, G.S., Impey, S. and Goodman, R.H. (2004) Cell-type-specific binding of the transcription factor CREB to the cAMP-response element. *Proc. Natl. Acad. Sci. U.S.A.*, **101**, 13572–13577.
17. Molina, C.A., Foulkes, N.S., Lalli, E. and Sassone-Corsi, P. (1993) Inducibility and negative autoregulation of CREM: an alternative promoter directs the expression of ICER, an early response repressor. *Cell*, **75**, 875–886.
18. Klejman, A. and Kaczmarek, L. (2006) Inducible cAMP early repressor (ICER) isoforms and neuronal apoptosis in cortical in vitro culture. *Acta Neurobiol. Exp. (Wars)*, **66**, 267–272.
19. Borlikova, G. and Endo, S. (2009) Inducible cAMP early repressor (ICER) and brain functions. *Mol. Neurobiol.*, **40**, 73–86.
20. Okoshi, R., Kubo, N., Nakashima, K., Shimozato, O., Nakagawara, A. and Ozaki, T. (2011) CREB represses p53-dependent reactivation of MDM2 through the complex formation with p53 and contributes to p53-mediated apoptosis in response to glucose deprivation. *Biochem. Biophys. Res. Commun.*, **406**, 79–84.
21. Gunning, P.W., Landreth, G.E., Layer, P., Ignatius, M. and Shooter, E.M. (1981) Nerve growth factor-induced differentiation of PC12 cells: evaluation of changes in RNA and DNA metabolism. *J. Neurosci.*, **1**, 368–379.
22. Michel, P.P., Vyas, S. and Agid, Y. (1995) Synergistic differentiation by chronic exposure to cyclic AMP and nerve growth factor renders rat pheochromocytoma PC12 cells totally dependent upon trophic support for survival. *Eur. J. Neurosci.*, **7**, 251–260.
23. Kim, D., Pertea, G., Trapnell, C., Pimentel, H., Kelley, R. and Salzberg, S.L. (2013) TopHat2: accurate alignment of transcriptomes in the presence of insertions, deletions and gene fusions. *Genome Biol.*, **14**, R36.
24. Wang, L., Wang, S. and Li, W. (2012) RSeQC: quality control of RNA-seq experiments. *Bioinformatics*, **28**, 2184–2185.
25. Zhang, Y., Liu, T., Meyer, C.A., Eeckhoutte, J., Johnson, D.S., Bernstein, B.E., Nusbaum, C., Myers, R.M., Brown, M., Li, W. *et al.* (2008) Model-based analysis of ChIP-Seq (MACS). *Genome Biol.*, **9**, R137.
26. Quinlan, A.R. and Hall, I.M. (2010) BEDTools: a flexible suite of utilities for comparing genomic features. *Bioinformatics*, **26**, 841–842.
27. Kong, L., Zhang, Y., Ye, Z.-Q., Liu, X.-Q., Zhao, S.-Q., Wei, L. and Gao, G. (2007) CPC: assess the protein-coding potential of transcripts using sequence features and support vector machine. *Nucleic Acids Res.*, **35**, W345–W349.
28. Sun, J., Nishiyama, T., Shimizu, K. and Kadota, K. (2013) TCC: an R package for comparing tag count data with robust normalization strategies. *BMC Bioinformatics*, **14**, 219.
29. Huang, D.W., Sherman, B.T. and Lempicki, R.A. (2009) Systematic and integrative analysis of large gene lists using DAVID bioinformatics resources. *Nat. Protoc.*, **4**, 44–57.
30. Zhu, L.J., Gazin, C., Lawson, N.D., Pagès, H., Lin, S.M., Lapointe, D.S. and Green, M.R. (2010) ChIPpeak Anno: a bioconductor package to annotate ChIP-seq and ChIP-chip data. *BMC Bioinformatics*, **11**, 237.
31. Mathelier, A., Zhao, X., Zhang, A.W., Parcy, F., Worsley-Hunt, R., Arenillas, D.J., Buchman, S., Chen, C.-Y., Chou, A., Jenasescu, H. *et al.* (2014) JASPAR 2014: an extensively expanded and updated open-access database of transcription factor binding profiles. *Nucleic Acids Res.*, **42**, D142–D147.
32. Kim, T.-K., Hemberg, M., Gray, J.M., Costa, A.M., Bear, D.M., Wu, J., Harmin, D.A., Laptewicz, M., Barbara-Haley, K., Kuersten, S. *et al.* (2010) Widespread transcription at neuronal activity-regulated enhancers. *Nature*, **465**, 182–187.
33. Lesiak, A., Pelz, C., Ando, H., Zhu, M., Davare, M., Lambert, T.J., Hansen, K.F., Obrietan, K., Appleyard, S.M., Impey, S. *et al.* (2013) A genome-wide screen of CREB occupancy identifies the RhoA inhibitors Par6C and Rnd3 as regulators of BDNF-induced synaptogenesis. *PLoS One*, **8**, e64658.
34. La Rocca, R., Fulciniti, M., Lakshmikanth, T., Mesuraca, M., Ali, T.H., Mazzei, V., Amodio, N., Catalano, L., Rotoli, B., Ouerfelli, O. *et al.* (2009) Early hematopoietic zinc finger protein prevents tumor cell recognition by natural killer cells. *J. Immunol.*, **182**, 4529–4537.
35. Shin, K.-J., Wall, E.A., Zavzavadjian, J.R., Santat, L.A., Liu, J., Hwang, J.-I., Rebres, R., Roach, T., Seaman, W., Simon, M.I. *et al.* (2006) A single lentiviral vector platform for microRNA-based conditional RNA interference and coordinated transgene expression. *Proc. Natl. Acad. Sci. U.S.A.*, **103**, 13759–13764.
36. Zufferey, R., Dull, T., Mandel, R.J., Bukovsky, A., Quiroz, D., Naldini, L. and Trono, D. (1998) Self-inactivating lentivirus vector for safe and efficient in vivo gene delivery. *J. Virol.*, **72**, 9873–9880.
37. Seila, A.C., Calabrese, J.M., Levine, S.S., Yeo, G.W., Rahl, P.B., Flynn, R.A., Young, R.A. and Sharp, P.A. (2008) Divergent transcription from active promoters. *Science*, **322**, 1849–1851.
38. Hu, H.Y., He, L. and Khaitovich, P. (2014) Deep sequencing reveals a novel class of bidirectional promoters associated with neuronal genes. *BMC Genomics*, **15**, 457.
39. Chang, J.H., Vuppalaanchi, D., van Niekerk, E., Trepel, J.B., Schanen, N.C. and Twiss, J.L. (2006) PC12 cells regulate inducible cyclic AMP (cAMP) element repressor expression to differentially control cAMP response element-dependent transcription in response to nerve growth factor and cAMP. *J. Neurochem.*, **99**, 1517–1530.
40. Osada, T., Kusakabe, H., Akutsu, H., Yagi, T. and Yanagimachi, R. (2002) Adult murine neurons: their chromatin and chromosome changes and failure to support embryonic development as revealed by nuclear transfer. *Cytogenet. Genome Res.*, **97**, 7–12.
41. Wakayama, T., Perry, A.C., Zuccotti, M., Johnson, K.R. and Yanagimachi, R. (1998) Full-term development of mice from enucleated oocytes injected with cumulus cell nuclei. *Nature*, **394**, 369–374.
42. Wakayama, T. and Yanagimachi, R. (1999) Cloning of male mice from adult tail-tip cells. *Nat. Genet.*, **22**, 127–128.
43. Lee, E.Y., Hu, N., Yuan, S.S., Cox, L.A., Bradley, A., Lee, W.H. and Herrup, K. (1994) Dual roles of the retinoblastoma protein in cell cycle regulation and neuron differentiation. *Genes Dev.*, **8**, 2008–2021.

44. Galderisi,U., Jori,F.P. and Giordano,A. (2003) Cell cycle regulation and neural differentiation. *Oncogene*, **22**, 5208–5219.
45. Lim,S. and Kaldis,P. (2012) Loss of Cdk2 and Cdk4 induces a switch from proliferation to differentiation in neural stem cells. *Stem Cells*, **30**, 1509–1520.
46. Yan,G.Z. and Ziff,E.B. (1995) NGF regulates the PC12 cell cycle machinery through specific inhibition of the Cdk kinases and induction of cyclin D1. *J. Neurosci.*, **15**, 6200–6212.
47. Yan,G.Z. and Ziff,E.B. (1997) Nerve growth factor induces transcription of the p21 WAF1/CIP1 and cyclin D1 genes in PC12 cells by activating the Sp1 transcription factor. *J. Neurosci.*, **17**, 6122–6132.
48. Dobashi,Y., Shoji,M., Kitagawa,M., Noguchi,T. and Kameya,T. (2000) Simultaneous suppression of cdc2 and cdk2 activities induces neuronal differentiation of PC12 cells. *J. Biol. Chem.*, **275**, 12572–12580.
49. Hayes,T.E., Valtz,N.L. and McKay,R.D. (1991) Downregulation of CDC2 upon terminal differentiation of neurons. *New Biol.*, **3**, 259–269.
50. Okano,H.J., Pfaff,D.W. and Gibbs,R.B. (1993) RB and Cdc2 expression in brain: correlations with 3H-thymidine incorporation and neurogenesis. *J. Neurosci.*, **13**, 2930–2938.
51. Shu,T., Tseng,H.-C., Sapir,T., Stern,P., Zhou,Y., Sanada,K., Fischer,A., Coquelle,F.M., Reiner,O. and Tsai,L.-H. (2006) Doublecortin-like kinase controls neurogenesis by regulating mitotic spindles and M phase progression. *Neuron*, **49**, 25–39.
52. Sigova,A.A., Mullen,A.C., Molinie,B., Gupta,S., Orlando,D.A., Guenther,M.G., Almada,A.E., Lin,C., Sharp,P.A., Giallourakis,C.C. *et al.* (2013) Divergent transcription of long noncoding RNA/mRNA gene pairs in embryonic stem cells. *Proc. Natl. Acad. Sci. U.S.A.*, **110**, 2876–2881.
53. Kapranov,P., Cheng,J., Dike,S., Nix,D.A., Duttagupta,R., Willingham,A.T., Stadler,P.F., Hertel,J., Hackermüller,J., Hofacker,I.L. *et al.* (2007) RNA maps reveal new RNA classes and a possible function for pervasive transcription. *Science*, **316**, 1484–1488.
54. Melgar,M.F., Collins,F.S. and Sethupathy,P. (2011) Discovery of active enhancers through bidirectional expression of short transcripts. *Genome Biol.*, **12**, R113.
55. Hah,N., Murakami,S., Nagari,A., Danko,C.G. and Kraus,W.L. (2013) Enhancer transcripts mark active estrogen receptor binding sites. *Genome Res.*, **23**, 1210–1223.
56. Kaikkonen,M.U., Spann,N.J., Heinz,S., Romanoski,C.E., Allison,K.A., Stender,J.D., Chun,H.B., Tough,D.F., Prinjha,R.K., Benner,C. *et al.* (2013) Remodeling of the enhancer landscape during macrophage activation is coupled to enhancer transcription. *Mol. Cell*, **51**, 310–325.
57. Lai,F., Orom,U.A., Cesaroni,M., Beringer,M., Taatjes,D.J., Blobel,G.A. and Shiekhattar,R. (2013) Activating RNAs associate with Mediator to enhance chromatin architecture and transcription. *Nature*, **494**, 497–501.
58. Andersson,R., Gebhard,C., Miguel-Escalada,I., Hoof,I., Bornholdt,J., Boyd,M., Chen,Y., Zhao,X., Schmidl,C., Suzuki,T. *et al.* (2014) An atlas of active enhancers across human cell types and tissues. *Nature*, **507**, 455–461.
59. Léveillé,N., Melo,C.A., Rooijers,K., Díaz-Lagares,A., Melo,S.A., Korkmaz,G., Lopes,R., Akbari Moqadam,F., Maia,A.R., Wijchers,P.J. *et al.* (2015) Genome-wide profiling of p53-regulated enhancer RNAs uncovers a subset of enhancers controlled by a lncRNA. *Nat. Commun.*, **6**, 6520.
60. Raemaekers,T., Ribbeck,K., Beaudouin,J., Annaert,W., Van Camp,M., Stockmans,I., Smets,N., Bouillon,R., Ellenberg,J. and Carmeliet,G. (2003) NuSAP, a novel microtubule-associated protein involved in mitotic spindle organization. *J. Cell Biol.*, **162**, 1017–1029.
61. Ribbeck,K., Raemaekers,T., Carmeliet,G. and Mattaj,I.W. (2007) A role for NuSAP in linking microtubules to mitotic chromosomes. *Curr. Biol.*, **17**, 230–236.
62. Vanden Bosch,A., Raemaekers,T., Denayer,S., Torrekens,S., Smets,N., Moermans,K., Dewerchin,M., Carmeliet,P. and Carmeliet,G. (2010) NuSAP is essential for chromatin-induced spindle formation during early embryogenesis. *J. Cell. Sci.*, **123**, 3244–3255.
63. Li,L., Zhou,Y., Sun,L., Xing,G., Tian,C., Sun,J., Zhang,L. and He,F. (2007) NuSAP is degraded by APC/C-Cdh1 and its overexpression results in mitotic arrest dependent of its microtubules' affinity. *Cell. Signal.*, **19**, 2046–2055.
64. Boque-Sastre,R., Soler,M., Oliveira-Mateos,C., Portela,A., Moutinho,C., Sayols,S., Villanueva,A., Esteller,M. and Guil,S. (2015) Head-to-head antisense transcription and R-loop formation promotes transcriptional activation. *Proc. Natl. Acad. Sci. U.S.A.*, **112**, 5785–5790.
65. Wang,K.C., Yang,Y.W., Liu,B., Sanyal,A., Corces-Zimmerman,R., Chen,Y., Lajoie,B.R., Protacio,A., Flynn,R.A., Gupta,R.A. *et al.* (2011) A long noncoding RNA maintains active chromatin to coordinate homeotic gene expression. *Nature*, **472**, 120–124.
66. Yang,L., Lin,C., Jin,C., Yang,J.C., Tanasa,B., Li,W., Merkurjev,D., Ohgi,K.A., Meng,D., Zhang,J. *et al.* (2013) lncRNA-dependent mechanisms of androgen-receptor-regulated gene activation programs. *Nature*, **500**, 598–602.
67. Puc,J., Kozbial,P., Li,W., Tan,Y., Liu,Z., Suter,T., Ohgi,K.A., Zhang,J., Aggarwal,A.K. and Rosenfeld,M.G. (2015) Ligand-dependent enhancer activation regulated by topoisomerase-I activity. *Cell*, **160**, 367–380.
68. Hilton,I.B., D'Ippolito,A.M., Vockley,C.M., Thakore,P.I., Crawford,G.E., Reddy,T.E. and Gersbach,C.A. (2015) Epigenome editing by a CRISPR-Cas9-based acetyltransferase activates genes from promoters and enhancers. *Nat. Biotechnol.*, **33**, 510–517.
69. Stasevich,T.J., Hayashi-Takanaka,Y., Sato,Y., Maehara,K., Ohkawa,Y., Sakata-Sogawa,K., Tokunaga,M., Nagase,T., Nozaki,N., McNally,J.G. *et al.* (2014) Regulation of RNA polymerase II activation by histone acetylation in single living cells. *Nature*, **516**, 272–275.
70. Ratmeyer,L., Vinayak,R., Zhong,Y.Y., Zon,G. and Wilson,W.D. (1994) Sequence specific thermodynamic and structural properties for DNA:RNA duplexes. *Biochemistry*, **33**, 5298–5304.
71. Roberts,R.W. and Crothers,D.M. (1992) Stability and properties of double and triple helices: dramatic effects of RNA or DNA backbone composition. *Science*, **258**, 1463–1466.

SCIENTIFIC REPORTS

OPEN

Identification of genes associated with the astrocyte-specific gene *Gfap* during astrocyte differentiation

Received: 23 January 2015

Accepted: 16 March 2016

Published: 04 April 2016

Kenji Ito¹, Tsukasa Sanosaka², Katsuhide Igarashi³, Maky Ideta-Otsuka³, Akira Aizawa¹, Yuichi Uosaki¹, Azumi Noguchi¹, Hirokazu Arakawa¹, Kinichi Nakashima² & Takumi Takizawa¹

Chromosomes and genes are non-randomly arranged within the mammalian cell nucleus, and gene clustering is of great significance in transcriptional regulation. However, the relevance of gene clustering and their expression during the differentiation of neural precursor cells (NPCs) into astrocytes remains unclear. We performed a genome-wide enhanced circular chromosomal conformation capture (e4C) to screen for genes associated with the astrocyte-specific gene glial fibrillary acidic protein (*Gfap*) during astrocyte differentiation. We identified 18 genes that were specifically associated with *Gfap* and expressed in NPC-derived astrocytes. Our results provide additional evidence for the functional significance of gene clustering in transcriptional regulation during NPC differentiation.

An increasing amount of evidence supports the importance of spatial organization of the genome in the nuclei of higher eukaryotes¹. Chromosomes and genes are non-randomly arranged and occupy preferential positions within the nucleus². Moreover, these arrangements are associated with gene regulation because the sub-nuclear positions of genes change along with alterations in their transcriptional states^{3–6}. For instance, in naïve CD4⁺T helper cells, there is an inter-chromosomal association between the regulatory region of the TH2 cytokine locus and the interferon γ (*Ifng*) promoter region, where both are repressed⁷. On the other hand, in erythroid cells, Klf1-regulated genes including globins preferentially associate at a limited number of transcriptional factories containing high levels of Klf1 once activated⁸. Other observations based on chromosome conformation capture (3C) and its derivative techniques (4C, 5C, ChIA-PET) have shown that gene associations play roles in transcriptional regulation^{9–12}. These techniques are essential for revealing three-dimensional information regarding the spatial proximity of DNA within the cell nucleus^{13,14}.

Neural precursor cells (NPCs) in the central nervous system can self-renew and differentiate into neurons mid-gestation, and then into astrocytes and oligodendrocytes only after late-gestation¹⁵. Differentiation of NPCs is temporally and spatially regulated by several factors including cytokines and epigenetic modifications^{16,17}. NPCs from mouse telencephalon at late gestation (e.g., embryonic day [E] 14.5) are competent to differentiate into astrocytes upon stimulation with leukemia inhibitory factor (LIF)^{18,19}. LIF activates the transcription factor STAT3, which then binds to the promoter of an astrocyte specific gene, glial fibrillary acidic protein (*Gfap*), to induce its expression^{19,20}. This is of great relevance in astrocytogenesis, since mice lacking a common receptor for LIF, gp130, are largely devoid of *Gfap*-positive astrocytes. These astrocytes show a lower ability to support the survival of neurons²¹. In addition, DNA demethylation and chromatin remodeling in STAT3 binding motifs on the *Gfap* promoter are essential for *Gfap* expression²².

Gfap gene loci have been shown to undergo a shift toward a more internal location upon transcriptional activation⁶. Furthermore, genomic regions adjacent to nuclear lamina are replaced as gene expression programs

¹Department of Pediatrics, Graduate School of Medicine, Gunma University, 3-39-22 Showa-machi, Maebashi, Gunma 371-8511, Japan. ²Stem Cell Biology and Medicine, Department of Stem cell Biology and Medicine, Graduate School of Medical Sciences, Kyushu University, 3-1-1 Maidashi, Higashi-ku, Fukuoka, 812-8582, Japan. ³Life Science Tokyo Advanced Research Center (L-Star), Pharmacy and Pharmaceutical Science, Hoshi University, 2-4-41 Ebara, Shinagawa-ku, Tokyo 142-5801, Japan. Correspondence and requests for materials should be addressed to T.T. (email: takizawt@gunma-u.ac.jp)

change during astrocyte differentiation from NPCs²³. This indicates robust conversion of genome localization during astrocytogenesis; however, little is known about the relevance of gene clustering in NPC differentiation.

In this study, we screened for genes that associate with *Gfap* during the astrocyte differentiation of NPCs by using enhanced circular chromosome conformation capture with minor modifications (modified e4C). We looked for a correlation between gene clustering and transcriptional activities by comparing data from modified e4C and expression arrays. We identified 18 genes associated with *Gfap* that are also expressed specifically in LIF-induced astrocytes. DNA fluorescence *in situ* hybridization (FISH) confirmed the clustering of some genes and *Gfap*. These findings support the possibility that the association of co-expressing genes is involved in astrocyte differentiation.

Results

Genome-wide screening of genes specifically associated with *Gfap* and expressed in NPC-derived astrocytes.

As a first step toward identifying genes clustered with and regulated similarly to *Gfap* during astrocyte differentiation, we decided to perform a modified e4C assay with a few modifications⁸. NPCs derived from E14.5 mouse brains can differentiate into astrocytes after being cultured *in vitro* for more than 4 days in the presence of the astrocyte-inducing cytokine LIF¹⁹. We isolated neuroepithelial cells from the telencephalon of E14.5 mice and cultured them for 5 consecutive days (designated as NPCs). After one passage, the NPCs were further cultured for 4 days with LIF to differentiate them into astrocytes (designated as LIF+ cells) (Fig. 1A). As reported previously, under these conditions, ~20% of NPCs differentiate into astrocytes as judged by immunofluorescence labeling of the astrocyte marker *GFAP* (Fig. 1B)^{6,19}. The NPCs grown in extended culture without LIF (LIF- cells) were also tested as a control (Fig. 1A,B).

As “bait” for the e4C assay, we used a genomic region containing a STAT3 cognate sequence on the *Gfap* promoter, the *Gfap* STAT3-binding site (GSBS). The GSBS is located ~1.5 kb upstream of the transcription start site and is a prerequisite for *Gfap* transcription during astrocytogenesis from NPCs¹⁹. We first tried *Bgl*III digestion of the flanking regions of GSBS. However, the digestion efficiency in this region as assessed with quantitative PCR was much lower in cells that did not express *Gfap* than those that did express *Gfap* (20.8% vs. 61.3%). We assumed the insufficient digestion was due to highly compacted chromatin around the GSBS in those cells²². To improve accessibility of restriction enzymes to the chromatin, we added an extra step of hydrochloric acid treatment to the original e4C protocol (Fig. 1C). Indeed, this achieved comparable digestion efficiency at the GSBS region in different types of cells (Fig. 1D) and helped to identify a large number of e4C peaks in both *cis* and *trans* in two biological replicates. As expected, many peaks were found around the bait locus, and the ratio between the e4C peak number and chromosome size was the highest for chromosome 11, which encodes *Gfap* in all the types of cells tested (Fig. 1E,F).

Trans-chromosomal interactions were also found in all types of cells tested (Fig. 2A). A number of positive probes were not replicated between two biological repeats (Figure S1A); this might be partly due to a resolution difference between the 3C assay and microarray probes. The former sometimes has cytological but not necessarily molecular resolution²⁴, while the arrays represent molecular resolution and contain a probe or two for most target fragments between *Bgl*III and *Nla*III with expected lengths within 200 bp (Figure S1B). Therefore, we only focused on replicated positive probes. The analysis of distances of positive probes from the nearest genes revealed that probes 10–30 kbp away from the transcriptional start or end sites were enriched with e4C compared to all probes on the array (Figure S2). Indeed, as many as ~1,000 genes were found within 50 kbp from the positive probes that we defined as being associated with *Gfap* in each cell type (Fig. 2B and Supplemental Table S2), likely because of the relatively lower resolution of the 3C or its derivative assay²⁴. Among them, 587 genes were associated with *Gfap* exclusively in LIF+ cells (Fig. 2B). We also found considerable overlap (564 genes) between NPCs and LIF- cells but less overlap between NPCs and LIF+ cells (430 genes) or LIF+ and LIF- cells (295 genes). These results show distinct associations between *Gfap* and other genes in LIF+ cells versus NPCs and LIF- cells.

To identify genes that are simultaneously associated with *Gfap* gene loci and expressed specifically in LIF+ cells, gene expression profiles in each cell type were examined by Affymetrix GeneChip analysis. To normalize gene expression levels from different samples, we adopted the PerCellome method, which provides “per cell” read-outs in copy numbers of mRNA by adding a set of external spike mRNAs in proportion to the DNA content as a substitute for the measurement of cell numbers in the sample²⁵. We found 2,083 genes in LIF+ cells and 2,404 in LIF- cells, with more than a two-fold increase in expression in NPCs. There were 1,132 overlapping genes between LIF+ and LIF- cells and 951 genes exclusively expressed in LIF+ cells (Fig. 2C and Supplemental Table S3). By referring to genes associated in LIF+ cells in the e4C assay, we found 18 genes that were associated with *Gfap* and expressed at particularly high levels in LIF+ cells (Table 1 and Fig. 2D).

Validation of GeneChip array and modified e4C results. Among the putative 18 genes, we selected *Ogn*, *Osmr*, *Ecr4*, *A2m*, and *Gab1* for further analysis because they have been implicated as playing important roles in the central nervous system^{26–30}. To affirm the results of the GeneChip analysis, we tested the expressions of the five genes and *Gfap* by RT-qPCR. As expected, mRNA expression levels of the six genes were all significantly increased 72 and 96 h after LIF stimulation (Fig. 3).

The long-range interactions identified by 4C technology need to be verified by completely independent methods such as FISH because 4C technology shows average chromosome conformations from millions of nuclei^{31,32}. Therefore, we next performed DNA FISH for each of the five putative associating genes (Fig. 4A and Figure S3). In addition to these five genes, we also tested genes that were negative in modified e4C and located on different chromosomes, namely *Ahnak* on chromosome 19 and *Nme8* on chromosome 13. The GeneChip analysis showed that *Ahnak* is exclusively expressed in LIF+ cells, while *Nme8* is expressed at miniscule levels in NPCs, LIF+, and LIF- cells. Three genes (*Ogn*, *Osmr*, and *Ecr4*) out of the five putative genes show a significant increase in the number of cells with associated alleles in the LIF+ culture (Fig. 4B). Although not significant, similar tendencies

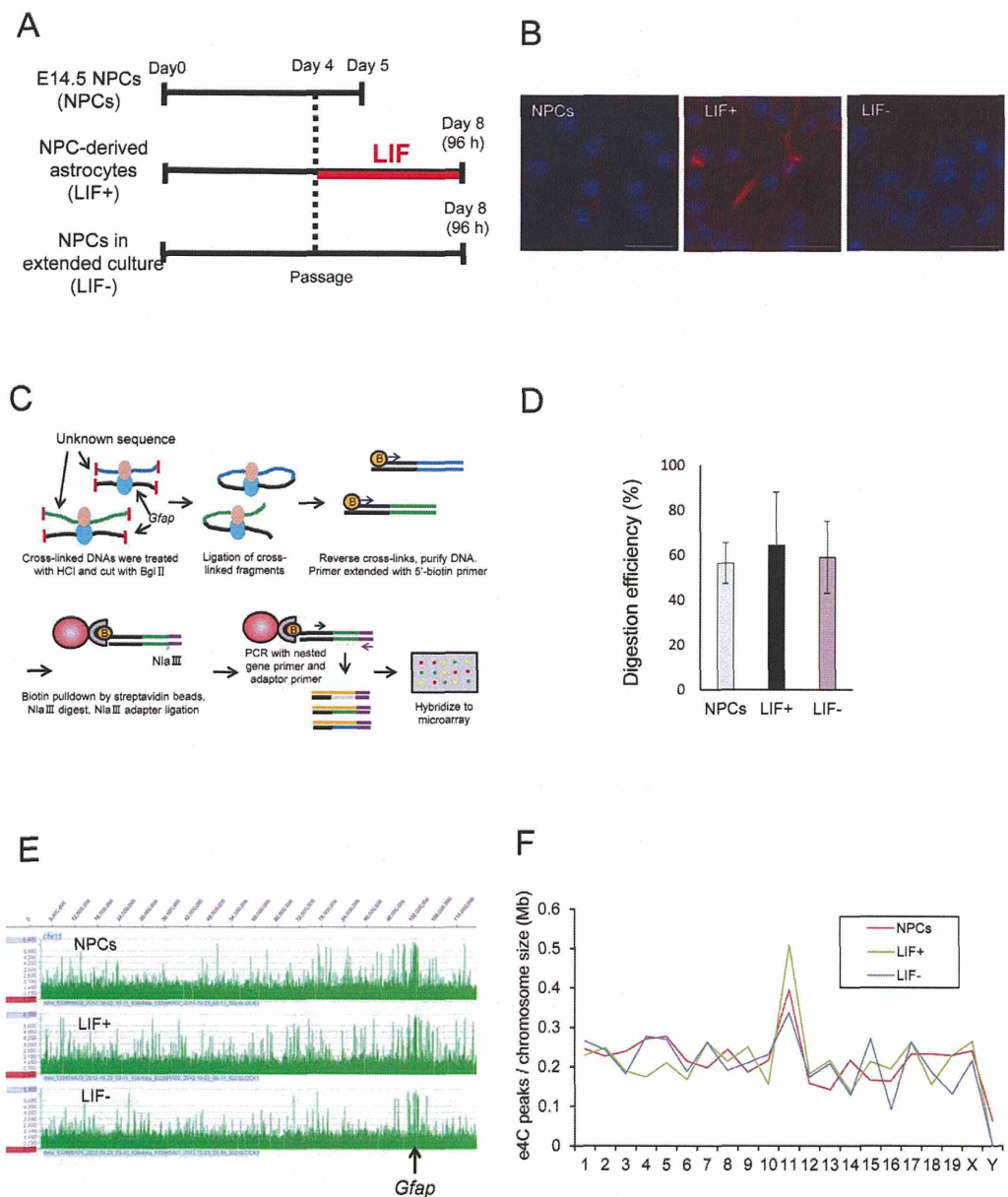


Figure 1. Genome-wide interactions of the *Gfap* loci in NPCs, LIF+, and LIF- cells. (A) Schematic experimental protocol. NPCs isolated from E14.5 mouse telencephalon were cultured and replated on day 4. On day 5, cells were used for experiments as NPCs. NPC-derived astrocytes and NPCs in extended culture were collected after an additional 4 days of culture with or without LIF. On day 8, the cells were used for experiments as LIF+ or LIF- cells. (B) NPCs, LIF+, and LIF- cells were stained with an anti-GFAP antibody (red, GFAP; blue, DAPI). Scale bar = 20 μ m. (C) Schematic representation of the modified e4C method. Chromatin was fixed in paraformaldehyde and treated with 0.1 N hydrochloric acid, then digested with *Bgl*II and ligated. The resulting hybrid molecules were used as a template for the primer extension reaction using the bait-specific primer. This was followed by adaptor ligation, nested PCR, labelling with fluorescent dye, and hybridization to a custom microarray. (D) The digestion efficiency of the DNA samples used for modified e4C. Relative amounts of PCR products on a *Bgl*II recognition site located near the *Gfap* STAT3 binding site (GSBS) are shown. (E) Association profiles were determined as the signal ratio of e4C samples to reference genomic DNA. $\text{Log}_2(\text{e4C DNA}/\text{genomic DNA}) = 2$ was set as a cut-off value. (F) Number of e4C peaks on each chromosome. Chromosome sizes were obtained from the Mouse Genome Browser Gateway (NCBI37/mm9).

were observed for *A2m* and *Gab1*. The number of cells with close proximity to *Gfap* did not change significantly for *Ahnak* and *Nme8* in different types of cells. Overall, there were no significant differences in the distribution of distances between *Gfap* and those gene loci among the three types of cells (Figure S4). We did notice a

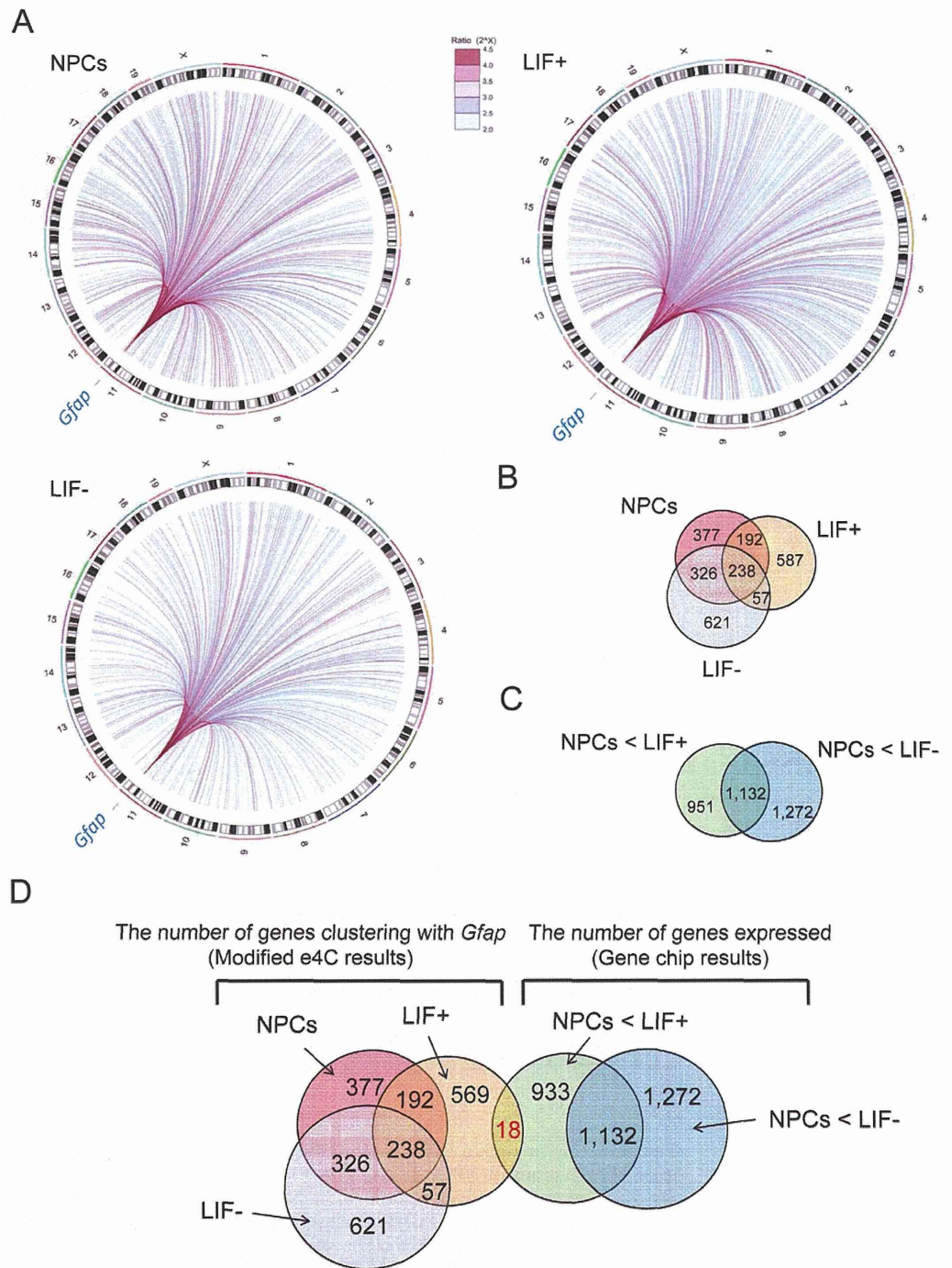


Figure 2. Identification of putative genes specifically associated with *Gfap* and expressed in LIF+ cells. (A) Circos plots showing interactions between the *Gfap* locus and interacting partners, with each line representing an interaction. Chromosomes are plotted along the circle. These plots were generated using the R package. The results of NPC, LIF+, and LIF- cells are shown separately. Each line color represents the ratios of intensities of peaks compared to genomic controls. (B) Venn diagram of the *Gfap*-associating *Bgl*III fragments from e4C results in NPC, LIF+, and LIF- cells. (C) Venn diagram of the genes expressed more highly in either LIF+ or LIF- cells than NPC. (D) Venn diagram of 587 genes specifically associated with *Gfap* in LIF+ cells and 946 genes specifically expressed in LIF+ cells.

consistent difference between NPC and LIF- in the association of each pair of probes (Fig. 4B). This was not explained by the nuclear diameter because it was not significantly different between NPC, LIF+, and LIF- cells

Accession	Gene symbol	NPCs	LIF+	LIF-	LIF+/NPCs	LIF-/NPCs	STAT3 binding site	Distance to probe region detected by e4C
NM_011019	<i>Osmr</i>	0.20	14.43	0.27	72.14	1.33	○	10–30 kb from TES
NM_008760	<i>Ogn</i>	0.10	3.46	0.04	34.58	0.42	○	10–30 kb from TSS
NM_011313	<i>S100a6</i>	1.20	29.50	1.27	24.58	1.06	○	10–30 kb from TES
NM_172471	<i>Itih5</i>	0.60	11.04	1.81	18.40	3.02	○	>30 kb from TES
NM_175459	<i>Glis3</i>	0.40	2.97	0.38	7.43	0.94	○	>30 kb from TSS
NM_008046	<i>Fst</i>	0.20	1.36	0.23	6.82	1.16	○	>30 kb from TES
NM_133832	<i>Rdh10</i>	1.20	4.97	1.76	4.14	1.47	○	5–10 kb from TSS
NM_024283	<i>Ecrge4</i>	0.50	1.76	0.08	3.52	0.16	○	>30 kb from TSS
NM_011883	<i>Rnfl3</i>	2.70	9.12	5.38	3.38	1.99	○	10–30 kb from TES
NM_175628	<i>A2m</i>	11.10	37.32	4.31	3.36	0.39	○	5–10 kb from TES
BC019423	<i>Rsph9</i>	0.80	1.99	0.61	2.48	0.76	×	10–30 kb from TES
BC110634	<i>Galntf1</i>	3.00	7.42	3.95	2.47	1.32	○	>30 kb from TES
NM_009011	<i>Rad23b</i>	6.00	14.72	11.27	2.45	1.88	×	>30 kb from TES
NM_009371	<i>Tgfb2</i>	1.00	2.33	0.29	2.33	0.29	○	>30 kb from TSS
NM_173876	<i>Clcn3</i>	3.30	7.38	6.31	2.24	1.91	○	<2 kb from TES
NM_175836	<i>Spnb2</i>	4.60	10.06	6.84	2.19	1.49	○	>30 kb from TSS
NM_008654	<i>Ppp1r15a</i>	1.00	2.14	1.34	2.14	1.34	×	>30 kb from TES
BC094659	<i>Gab1</i>	11.70	23.66	11.72	2.02	1.00	×	2–5 kb from TES

Table 1. List of the 18 putative genes specifically associated with *Gfap* and expressed in LIF+ cells. TSS; transcription start site, TES; transcription end site.

($10.4 \pm 1.5 \mu\text{m}$ in NPCs, $10.1 \pm 1.1 \mu\text{m}$ in LIF+, and $10.2 \pm 1.2 \mu\text{m}$ in LIF-). LIF- is an extended culture of NPCs, which readily differentiate into astrocytes with changes in epigenetic programs dedicated to astrocytes^{19,33}. This might explain the constant difference between NPCs and LIF-. Consequently, these cell-based analysis results agree with the e4C findings.

Detailed gene association analysis. We previously reported that *Gfap* is expressed in a random mono-allelic manner in LIF+ cells and cortical astrocytes⁶. Hence, we investigated whether the alleles that associate are preferentially expressed with a simultaneous RNA/DNA-FISH assay. We used a probe targeting mature *Gfap* transcripts and probes targeting *Gfap* and *Ogn* gene loci. A significantly larger number of active *Gfap* alleles associated with *Ogn* loci than inactive ones (Fig. 5A,B). The results suggest that *Gfap* transcriptional activity is at least partially correlated with gene association.

According to the position weight matrix of STAT3 derived from the previous ChIP-seq data³⁴, there are STAT3 binding motifs within 5 kb of the transcription start sites of 14 of the 18 genes screened with the e4C (Table 1). This indicates that these genes are activated by the common transcription factor, STAT3. We therefore aimed to determine whether the genes with STAT3 binding motifs share the same locale, i.e. a transcription factory. We performed a multicolor DNA FISH assay using probes targeting *Gfap*, *Ogn*, and *Osmr*. We did not observe these three genes clustered in our system (Fig. 5C,D), indicating that these gene associations did not simultaneously occur.

In addition, a detailed analysis of the e4C results did not indicate direct interaction among the promoters of those genes; positive probes for those 18 genes were not mapped on the promoter regions (Table 1).

Discussion

In this study, we identified 18 genes that are specifically expressed and associated with the astrocyte-specific gene *Gfap* in NPC-derived astrocytes (LIF+ cells) by comparing gene association data obtained by applying a modified e4C genome-wide screening method to genome-wide gene expression profiles obtained from a microarray analysis. Importantly, these results were reproducible with two additional independent and distinct methods: DNA FISH and RT-qPCR. We also showed that the association of these genes correlated with *Gfap* transcriptional activity (Fig. 5A,B).

Long-range chromatin interactions including gene clustering are increasingly being recognized as an important mechanism to regulate gene expression. In many instances, these multi-gene complexes are hypothesized to be organized within “transcription factories” containing RNA polymerase II (RNAPII) and other components involved in transcription^{5,8,35}. Furthermore, most genes in these transcription factories are transcribed cooperatively, and some of these genes can influence each other³⁶. Although we need to investigate further to reveal the functional significance of clustering, the 18 genes identified in this study may have roles in regulating *Gfap* expression and astrocyte differentiation. In fact, one of the identified genes, *Osmr*, encodes an oncostatin M (OSM) receptor known to be involved in STAT3 activation and subsequent *Gfap* expression during astrocyte differentiation³⁷. The OSMR is essential for OSM, a member of the interleukin (IL)-6 family of cytokines, to activate downstream JAK-STAT signaling pathways by forming a heterodimer with the common signal transducer gp130. Interestingly, *Osmr* itself is transcriptionally activated by STAT3^{38,39}. This suggests that STAT3 may be involved in gene associations between *Gfap* and *Osmr*, and that the association has roles in initiating enhanceosomes for

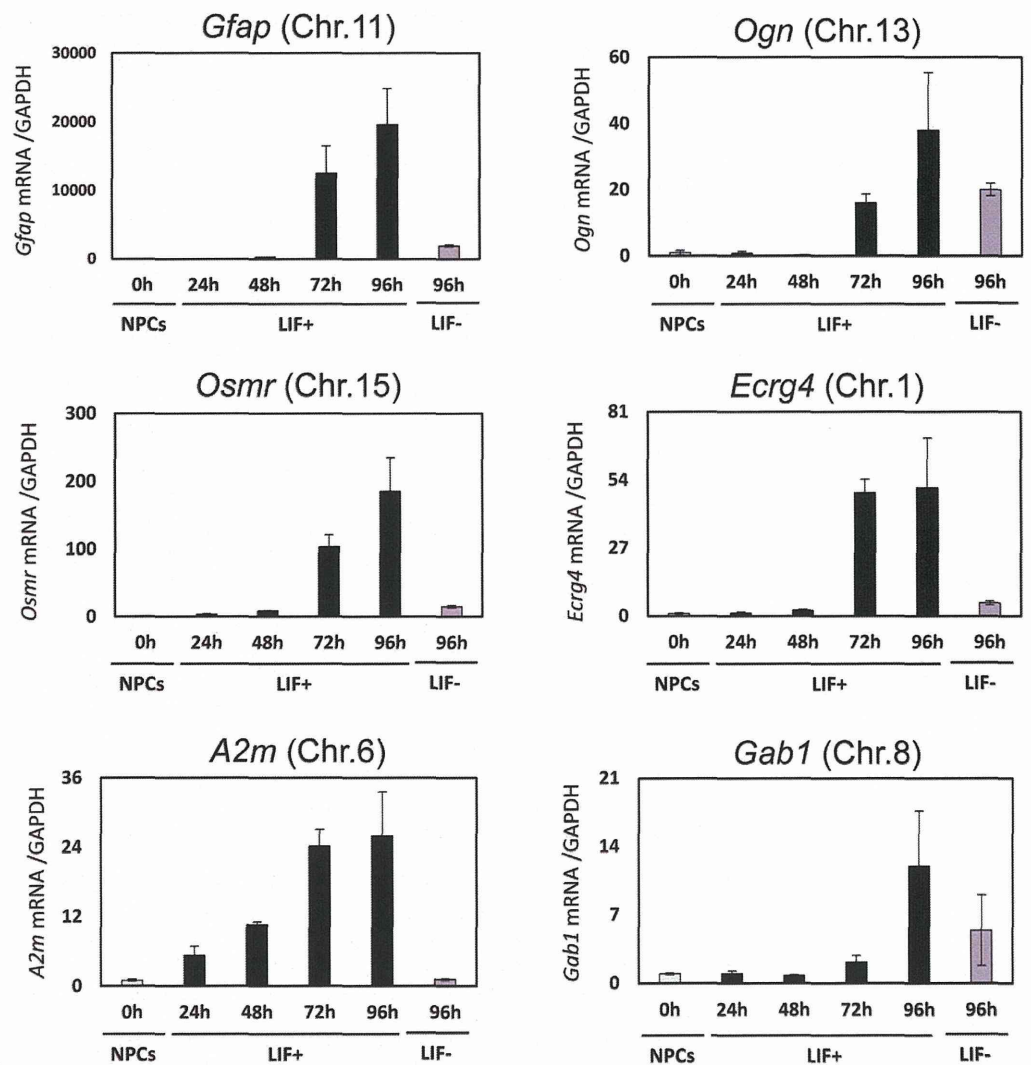


Figure 3. Validation in expression of *Gfap* and five putative genes identified by Genechip and modified e4C. Quantitative RT-PCR was performed on *Gfap* and five genes selected from modified e4C. The expression level of each gene was determined in NPCs (NPCs 0h), cells stimulated with LIF for different periods of time (LIF+ 24h, 48h, 72h, 96h), and without LIF (LIF- 96h). The results were normalized to *Gapdh* expression. Each graph represents the mean (\pm SEM) relative amount (compared with NPCs) in at least three experiments.

Gfap expression and astrocyte differentiation. Another identified gene, *Ecrq4*, participates in NPC cell cycle arrest through a mechanism involving the proteasome-dependent degradation of cyclins D1 and D3^{27,40}. Gene associations between *Gfap* and *Ecrq4* may be relevant for the appropriate timing of transcription initiation and astrocyte differentiation. On the other hand, e4C-positive probes were not found around the STAT3 binding sites of the 14 genes that possessed them. This indicates that close proximity of those genes, but not direct association of STAT3 binding sites, may play a role in enhancing transcription. It might be interesting to perform higher molecular resolution tests such as sequential chromatin immunoprecipitation to study gene interactions.

Changes in gene clustering reflect a wide range of genome functions such as replication, imprinting, and transcription^{41–43}. Although we revealed transcription-related gene associations of *Gfap*, transcription is not the only factor governing associations between *Gfap* and other genes. *Gfap* is monoallelically expressed in primary astrocytes and asymmetrically replicated, as are a number of other monoallelically expressed genes⁶. Furthermore, the reduction of transcription-repressive histone modifications (e.g., methylation of H3 at lysine 9 [H3K9me2, 3]) and the expansion of transcription-permissive histone modifications (e.g., methylation of H3 at lysine 4 [H3K4me3] and acetylation of H3 at lysine 9 [H3K9Ac] at GSBS) are important for *Gfap* expression^{44–46}. These previous findings support the idea that changes in the pairing of associated genes may depend not only on transcriptional activities but also on replication timing and epigenetic modifications. In fact, during differentiation of embryonic stem cells (ESCs) to NPCs, switching of chromosomal domains between early and late replication in the S-phase results in changes in gene pairings⁴³. Furthermore, proteins that bind to H3K27me3 and cause DNA